

A Lung Volume-Based Perfusion SPECT and CT Comparison Algorithm for Enhanced Pulmonary Embolism Diagnosis

1st Daniel Kisiel

Faculty of Electrical Engineering
Warsaw University of Technology
Warsaw, Poland
daniel.kisiel.stud@pw.edu.pl

2nd Eryk Muchorowski

Faculty of Electrical Engineering
Warsaw University of Technology
Warsaw, Poland
eryk.muchorowski.stud@pw.edu.pl

3rd Radosław Roszczyk

Faculty of Electrical Engineering
Warsaw University of Technology
Warsaw, Poland
radoslaw.roszczyk@pw.edu.pl

Abstract—Perfusion SPECT is a medical imaging modality often used alongside other techniques to diagnose pulmonary embolism. In this article, we developed a method that enables the calculation of the ratio between the lung volume derived from the SPECT examination and that obtained from a regular CT scan. This value allows for the quantification of lung regions with impaired perfusion. To compute this metric, it was necessary to segment the lung images from both examinations. For the CT images, we utilized an off-the-shelf algorithm based on U-Net architecture, whereas for the SPECT images, a fixed threshold determined empirically was applied. The subsequent step involved calculating the volume based on the associated metadata from the DICOM files. In a dataset comprising five patients (two healthy and three diseased), the developed algorithm flawlessly distinguished between the two groups. Thus, this method enables the determination of a precise numerical metric quantifying the severity of potential pulmonary embolism.

Index Terms—segmentation, pulmonary embolism, volume calculation, SPECT, CT

I. INTRODUCTION

A. Context - Pulmonary Embolism

Pulmonary Embolism (PE) is reported to be one of the most common cardiovascular diseases with the general annual occurrence rate in range from 39-115 per 100 000 population. It is caused by a blood clot that develops in a blood vessel elsewhere in the body and travels to an artery in the lung, forming a blockage [1], as presented on Fig. 1.

B. Diagnosis - SPECT

Lung V/Q (ventilation/perfusion) SPECT is one of an established diagnostic imaging test for suspected PE. The idea behind this test is to use radioactive tracer applied intravenous (perfusion) or by inhalation (ventilation). Afterwards, a gamma camera is used to detect the radiation emitted. The perfusion scan may exclude PE, however if its abnormal, then a ventilation scan should be considered for the interpretation (looking for so-called V/Q mismatch - preserved ventilation and absent perfusion, that implies potential PE). The regular CT is also often performed to improve diagnosis sensitivity and specificity [3]. All those results are then interpreted by a physician.

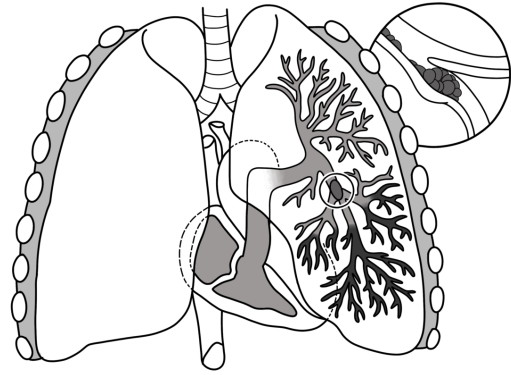


Fig. 1. Pulmonary Embolism - artery blockage [2]

C. Contribution

In this research we developed an algorithm for automatic comparison between Perfusion SPECT and regular CT examinations. The key idea is to estimate lung volumes from those two examinations, calculating the ratio V_P/V_{CT} (Perfusion lung volume to CT lung volume). The assumption is that its low value may indicate there are some regions without perfusion, thus patient may suffer from PE (similar like in V/Q mismatch approach). This algorithm may enhance PE diagnosis sensitivity and specificity. It also introduces a metric quantifying the severity of potential PE calculated automatically.

II. MATERIALS AND METHODS

A. Problem Formulation

Given patient's imaging data from Perfusion SPECT and Regular CT, our objective is to estimate lungs volume from both examinations. With such calculated volumes, it will be possible to calculate V_P/V_{CT} ratio. This numeric value describes how much of the lungs has present perfusion (referencing to theoretical volume from CT scan). Near-one values

indicate fully preserved perfusion, while lower suggest absent perfusion in some lung segments. It is worth noticing that such method has some variability due to unpredictability of radioactive tracer distribution and its permeability (situation, when radioisotope penetrates through the lung tissue). However, our target is to find certain threshold that will allow us to separate PE-diseased and healthy patients preserving highest possible sensitivity and specificity.

B. Materials

The dataset included 5 patients, 3 of whom were diagnosed with PE and 2 healthy controls. For every patient, the following data was available:

- A series of CT scans in the lung window (axial view) with various number of slices, each with a resolution of 512x512
- A series of Perfusion SPECT scans (axial view), comprising 128 slices, each with a resolution of 128x128

The examinations were conducted using the *SIEMENS Symbia T6* diagnostic equipment. This data was provided in DICOM (Digital Imaging and Communications in Medicine) file format with all required metadata, especially:

- **Pixel Spacing and Slice Thickness** - parameters describing physical voxel size
- **Rescale Slope and Rescale Intercept** - values to convert stored pixel values into Hounsfield Units
- **Modality, Series Number, Instance Number** - to correctly group and order scans

C. General approach

Perfusion/CT ratio calculation is multi-stage process with following steps:

- 1) Acquisition and processing of DICOM files containing both CT and SPECT imaging data along with their associated metadata
- 2) Segmentation of SPECT images using a standardized fixed threshold method
- 3) Preparation of CT images for segmentation, including conversion of pixel values to HU
- 4) Application of an established segmentation algorithm to the CT images
- 5) Calculation of volumes for both imaging modalities using the physical voxel dimensions
- 6) Computation of the Perfusion/CT ratio based on the calculated volumes

All those steps were taken using Python programming language with necessary external libraries.

D. SPECT segmentation

The segmentation of SPECT images creates significant challenges compared to CT segmentation. While CT images provide clear anatomical boundaries based on tissue density differences (and can be clearly segmented thanks to Hounsfield Units), SPECT images represent data with gradual transitions, often grainy and contain regions with low or absent uptake that are still anatomically part of the organ.

Our approach to SPECT segmentation involves the following steps:

- **Data Preparation:** First, DICOM files containing SPECT imaging data are loaded. Perfusion SPECT images are processed.
- **Image Normalization:** Each image volume is normalized by dividing all voxel values by the maximum intensity value in the respective dataset. This standardizes the intensity range to [0,1] and enables consistent threshold application across different scans.
- **Threshold-based Segmentation:** A fixed threshold method is applied to the normalized images. After analysis of the image histograms and produced results across multiple samples, a threshold value of 0.1 (10% of maximum intensity) was selected. This threshold represents a compromise between including low-uptake regions and excluding background noise of the image.

The selection of 0.1 as the threshold was not arbitrary, but was based on our empirical tests. Note that this is a limitation of our approach, as no single threshold value can optimally segment all SPECT images because of the variability in the distribution of radioactive pharmaceuticals. Segmentation result is presented on Fig. 2. Despite it may look like threshold was set too low, this inaccuracy does not affect our methodology, since it is calculated in the same way for every patient.

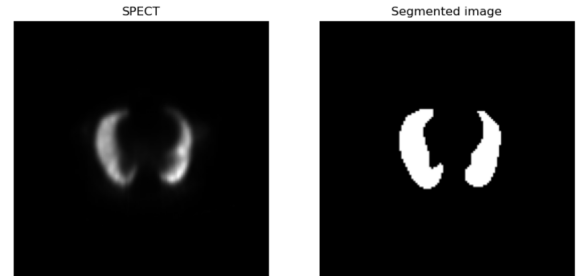


Fig. 2. SPECT slice segmentation

E. Alternative SPECT segmentation

During our analysis of the segmentation problem, we conducted a literature review to identify key existing approaches. The most notable methods are outlined in the following summary.

- **Active Shape Models (ASM):** ASM trained on reference CT lung shapes [4] can be applied to SPECT images. This method incorporates anatomical knowledge to overcome the limitations of intensity-based segmentation, especially in regions with perfusion defects.
- **CNN-based Segmentation:** More recently, some researchers demonstrated the effectiveness of convolutional neural networks for automated segmentation of the lungs, liver, and tumors from SPECT/CT images [5].
- **Registration-Based Methods:** Several researchers [6] have used co-registration of CT and SPECT images, using

the anatomical information from CT to guide SPECT segmentation.

Although our fixed threshold method (10% of minimum intensity) used in this study is adequate for research purposes it has significant limitations. Our approach does not adapt to the specific characteristics of individual images, which becomes problematic with variations in radio pharmaceutical uptake, patient physiology, and acquisition parameters. For future implementations, more sophisticated segmentation methods would be recommended, particularly those incorporating anatomical knowledge (such as active shape models) or deep learning approaches capable of capturing complex patterns from training data.

It is also worth mentioning, that data distribution in SPECT examination does not allow finding any reliable threshold with standard methods like ie. Otsu's thresholding. Looking at histogram presented at Fig. 3 (logarithmic scale), we can see that the data distribution have continuous characteristics so it isn't possible to simply extract two classes (background and tissue).

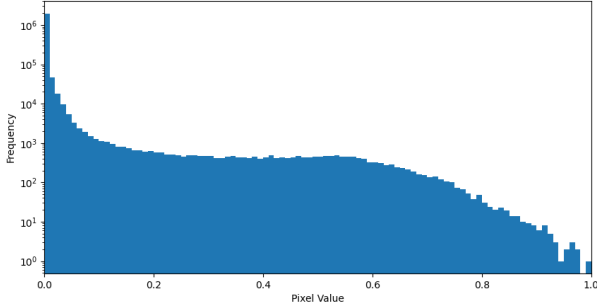


Fig. 3. SPECT pixel value distribution

F. CT segmentation

All dicom files were processed using **pydicom** library. The imaging data was represented as a 3D **numpy** array. The first step was to transpose pixel values into Hounsfield Units (which is required by the segmentation algorithm). It can be done with associated dicom metadata using the formula for each pixel value px_{val} :

$$HU = RescaleSlope \cdot px_{val} + RescaleIntercept \quad (1)$$

The result of this operation is again 3D numpy array in HU representation.

Such prepared volume was then segmented using **lungmask** [7] library. It implements an U-Net based deep learning approach to lung segmentation specifically designed for CT images. This model was trained on a diverse dataset of chest CT scans and has been demonstrated to be robust across various scanning protocols and pathologies. The segmentation process automatically identifies and labels voxels as either lung tissue or background, producing a binary mask of the same dimensions as the input volume. The final output was a

3D binary mask where voxels with value 1 represent lung tissue and 0 represent non-lung regions. Fig. 4 represents segmentation result for a one slice.

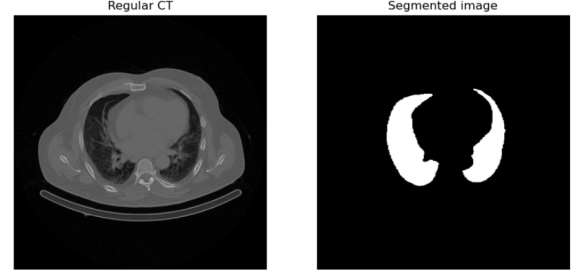


Fig. 4. CT slice segmentation

G. Volume and ratio calculation

Having segmented both volumes (SPECT and CT) we were able to calculate estimated lung volumes from both scans. To begin with, we needed to obtain real pixel dimensions from associated dicom metadata. The three dimensions can be found in Pixel Spacing (2-element tuple) and Slice Thickness (single value). Important notice is that the value of one dimension of voxel is equal to Slice Thickness due to the fact Spacing Between Slices is 0 in our case. The next step was to simply count 1's voxels in both segmented scans and multiply it by the corresponding real voxel volumes.

III. RESULTS AND DISCUSSION

A. Output

The obtained results are presented in the Tab I, where 'D' stands for diseased and 'H' for healthy patients. It contains lung volumes (in liters) from CT and SPECT examinations and the calculated ratio V_P/V_{CT} .

As expected, for healthy patients, calculated volume ratio is greater than for diseased ones. The algorithm was able to fully separate diseased and healthy controls. The difference between group boundaries ($\mu_{Hmin} - \mu_{Dmax}$) is equal to 0.174. The difference between group mean values ($\mu_{Havg} - \mu_{Davg}$) is equal to 0.281.

The next step is to determine the best value for threshold. The most basic approach would be to define its value as $T = \frac{\mu_{Hmin} + \mu_{Dmax}}{2}$ - middle point between boundary values. For the provided data, the threshold value would be 0.782. However, more data are required to find a reliable threshold. In case two classes overlaps, another method, that minimizes misclassification (number of controls classified incorrectly), is needed.

TABLE I
RATIO RESULT TABLE

Patient	CT	SPECT	Ratio
D1	4.204	2.918	0.694
D2	5.496	2.954	0.537
D3	3.110	2.162	0.695
H1	3.347	3.271	0.977
H2	2.407	2.091	0.869

B. Visualisation

All the visualisations are prepared using **Slicer** software. The pale purple model depicted in Fig. 5 represents the CT-generated lung reconstruction, while the overlaid gray model illustrates the SPECT data. This example, showcased using a healthy subject, demonstrates congruence between the two imaging modalities. The near-identical morphology of both models highlights the precision of the imaging techniques when applied to normal lung anatomy.

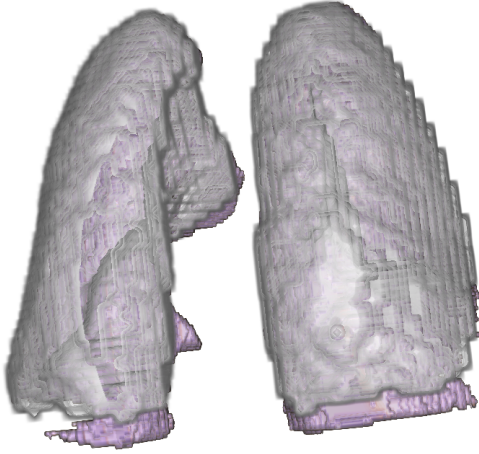


Fig. 5. 3D models of segmented SPECT and CT overlaying

Fig. 6 presents an alternative visualization of the same models. In this representation, the CT data was segmented using the **MONAI Auto3DSeg** model, complemented by SPECT data (not segmented). The SPECT information appears as a dark, luminous glow around the segmented structure, with notable protrusions visible in certain regions. This visualization approach offers a different perspective on the relationship between the anatomical (CT) and functional (SPECT) imaging data.

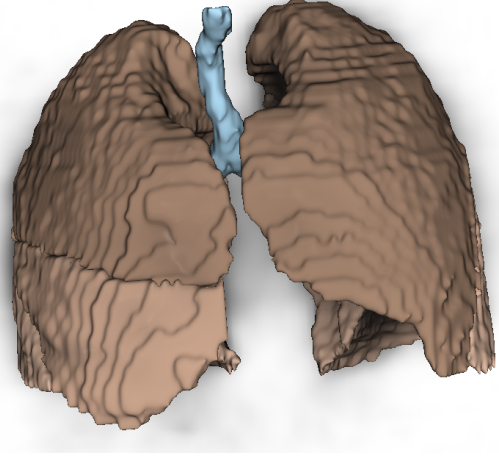


Fig. 6. 3D models reconstructed with MONAI

C. Performance tests

We consider the execution time of the proposed algorithm a critical factor, particularly because PE is a medical emergency that requires rapid diagnosis. Moreover, many hospitals operate with legacy hardware infrastructure.

With the exception of the CT segmentation process, the execution time for all other steps of the algorithm is negligible. In this section, we focus on measuring the time required to complete the CT segmentation step. The benchmark setup is presented below:

- AMD Ryzen 5 5600 6-Core Processor 3.50 GHz
- 32GB RAM
- Windows 11 x64
- No GPU acceleration

The tests involved segmenting five CT examinations, averaging approximately 140 slices each. The average segmentation time was **48s**. While GPU acceleration could significantly reduce this time, it is not universally supported across all hardware configurations.

IV. CONCLUSION

Although results are really promising, more data are required for a more reliable algorithm evaluation. It would be useful to establish fundamental metrics such as intra-class variance, sensitivity, specificity (in case classes overlaps). Also more data would allow to determine more reliable threshold value. What is more, it would be beneficial to introduce additional thresholds that would allow to divide patient into groups based on the eventual PE severity (ie. acute, low, none).

Future improvements might involve implementing more accurate SPECT segmentation algorithm to achieve more reliable results. It would also be beneficial to optimize the CT segmentation method, as it is currently quite time-consuming.

V. ACKNOWLEDGMENT

The authors wish to express their sincere appreciation to Warsaw Military Institute of Medicine for providing the data and for their effort in its interpretation and labeling. Their

contribution was instrumental in the analysis and development of this work. Additionally, the authors are grateful to them for suggesting the research topic, which played a crucial role in shaping the direction of this study.

VI. ACCESS

The code of presented algorithm can be accessed on Github [https://github.com/Ixico/lungs]. We need to know whether data also can be published (maybe it can since it's fully anonymized).

REFERENCES

- [1] A. C. Clark, J. Xue, and A. Sharma, 'Pulmonary Embolism: Epidemiology, Patient Presentation, Diagnosis, and Treatment', *Journal of Radiology Nursing*, vol. 38, no. 2, pp. 112–118, Jun. 2019, doi: 10.1016/j.jradnu.2019.01.006.
- [2] 'Pulmonary embolism, (accessed Mar. 31, 2025) - Wikipedia.' Available: https://en.wikipedia.org/wiki/Pulmonary_embolism
- [3] M. Bajc, J. B. Neilly, M. Miniati, C. Schuemichen, M. Meignan, and B. Jonson, 'EANM guidelines for ventilation/perfusion scintigraphy: Part 1. Pulmonary imaging with ventilation/perfusion single photon emission tomography', *Eur J Nucl Med Mol Imaging*, vol. 36, no. 8, pp. 1356–1370, Aug. 2009, doi: 10.1007/s00259-009-1170-5.
- [4] G.-A. Cheimariotis et al., 'Automatic lung segmentation in functional SPECT images using active shape models trained on reference lung shapes from CT', *Ann Nucl Med*, vol. 32, no. 2, pp. 94–104, Feb. 2018, doi: 10.1007/s12149-017-1223-y.
- [5] A. Chaichana et al., 'Automated segmentation of lung, liver, and liver tumors from Tc-99m MAA SPECT/CT images for Y-90 radioembolization using convolutional neural networks', *Medical Physics*, vol. 48, no. 12, pp. 7877–7890, 2021, doi: 10.1002/mp.15303.
- [6] S. Gupta, P. Gupta, and V. S. Verma, "Study on anatomical and functional medical image registration methods," *Neurocomputing*, vol. 452, pp. 534–548, Sep. 2021, doi: 10.1016/j.neucom.2020.08.085.
- [7] J. Hofmanninger, F. Prayer, J. Pan, S. Röhrich, H. Prosch, and G. Langs, 'Automatic lung segmentation in routine imaging is primarily a data diversity problem, not a methodology problem', *European Radiology Experimental*, vol. 4, no. 1, p. 50, Aug. 2020, doi: 10.1186/s41747-020-00173-2.